Magnetoplasmons of the Two-Dimensional Electron Grid

G. Y. Wu* and Y. Zhao
Department of Electrical Engineering, Princeton University, Princeton, New Jersey 08544
(Received 4 February 1993)

We present a theory of the magnetoplasmons of two-dimensional electron grid (antidot) structures. We develop a variational Wigner-Seitz model to study such periodic electron structures. We derive an analytical solution for the far-infrared (FIR) response, and obtain results in quantitative agreement with experiments. Our work provides not only an explanation for the recently observed FIR anomaly, but also a useful basis for further theoretical studies of collective properties of electron grid (antidot) structures.

PACS numbers: 72.15.Rn, 73.20.Dx, 73.20.Mf

The physics of two-dimensional electron gas (2DEG) has been a subject of great interest. With the advancement of microstructure technology, the study of the 2DEG has progressed to that of lateral superlattices (LSLs). For these many-electron systems, while the long-wavelength dynamic response of the uniform 2DEG and the LSLs of quantum wires and dots can largely be described by using the single-particle picture based on the Kohn theorem [1], the LSLs of grids (antidots) show many peculiarities in the magneto-optical [2,3] and magnetotransport measurements [4]. In the recent far-infrared (FIR) studies of the grid structure, Kern *et al.* [2] and Zhao *et al.* [3] observed, in the presence of magnetic field B, new resonances ν_+ and ν_- in addition to the electron cyclotron resonance (CR). They show an anomalous level-crossing-like feature in the ν-B dispersion, which was attributed to the breakdown of Kohn's theorem [3]. The high-frequency ν_+ branch starts at small B with a negative slope, and then increases in frequency with B, eventually approaching the CR. A second low-frequency ν_- branch begins with zero frequency at $B=0$, rises with B, and shows a slightly negative slope at high B. Moreover, the oscillator strength transfers from the ν_- mode to the ν_+ with increasing B, suggesting a mixing between the ν_- and the ν_+ modes. On the other hand, the foregoing anomaly has not been experimentally observed or theoretically predicted in similar studies of the 2D structures where the Kohn theorem holds [5–8]. Therefore, the grid (antidot) structures constitute interesting systems to study. In this Letter, we present a theory of the magnetoplasma modes and the FIR response of the grid (antidot) structure, and compare our model directly with the experiments. Our work provides not only an explanation for the observed FIR anomaly [2,3], but also a useful basis for further theoretical studies of collective properties of electron grid (antidot) structures.

We picture the system as a thin layer of 2DEG situated at the heterostructure interface (with the coordinate $x=0$) with a square lattice of antidots, which are high potential barriers impenetrable to electrons. The structure is bounded between two metal gates located at $x=x_1$ and x_2. The magnetic field B is taken to be along the x axis. Consistent with the experiments, we shall assume the length scales $\lambda \approx d \gg r_s$, where λ is the wavelength of the electron density oscillation, d is the lattice constant of the antidot array, and r_s is the interelectron spacing. The physics of long-λ plasma modes belongs to the continuum limit. In the present theory, we focus on the coarse-grain averages of the electron density fluctuation, the electric potential fluctuation, and the velocity field, $n(\boldsymbol{\rho},t)$, $V(\boldsymbol{\rho},x,t)$, and $\mathbf{v}(\boldsymbol{\rho},t)$, where $\boldsymbol{\rho}$ is a position vector on the y-z plane. We look for the normal modes with $n(\boldsymbol{\rho},t)=n(\boldsymbol{\rho})e^{-i\omega t}$, $V(\boldsymbol{\rho},x,t)=V(\boldsymbol{\rho},x)e^{-i\omega t}$, and $\mathbf{v}(\boldsymbol{\rho},t)=\mathbf{v}(\boldsymbol{\rho})e^{-i\omega t}$. They satisfy the Poisson equation and the plasma equation [5–7]

$$\nabla_2^2\left(\frac{n_s e}{m}V_0\right)+(\omega_c^2-\omega^2)n=0\,, \tag{1}$$

where V_0 is the potential fluctuation at the $x=0$ plane, n_s is the average electron density, ω_c is the CR frequency, and ∇_2^2 is the 2D Laplacian [9].

We propose a variational Wigner-Seitz (WS) model, which reduces the complicated problem to essentially that of a (circular) WS cell, and treats the intracell and intercell Coulomb interactions. The plan is to study the so-called screened limit first, and to use it as a guideline for setting up a model later for the general situation where the Coulomb interactions are important.

In the screened limit, e.g., $x_1 \to 0$, Coulomb interactions in the 2DEG are reduced by the metal gate. In this limit, one can picture it as a pair of parallel plates, i.e., a capacitor, with the upper end grounded. This capacitor approximation results in a local linear relationship between V_0 and n, with $V_0=-ex_1n/\varepsilon_1$, where ε_1 is the dielectric constant of the upper layer of the heterostructure. With this relation, the number of unknowns is reduced. For the periodic array of antidots, we write with the Bloch theorem $n(\boldsymbol{\rho})=e^{i\mathbf{q}\cdot\boldsymbol{\rho}}n_c(\boldsymbol{\rho})$, where $\mathbf{q}$ is a wave vector and n_c is cell periodic. For the present problem, it suffices to focus on the $\mathbf{q}=0$ solutions, since these are the modes excited by the FIR, which has a very long wavelength compared to the lattice constant of the array. The Bloch theorem transforms the many-cell problem to a one-cell one. However, the reduced problem requires the additional specification of boundary condition at the cell

0031-9007/93/71(13)/2114(4)$06.00

boundary. We derive it by adopting the idea of the WS method [10]. First, we approximate the WS unit cell as a circular disk, thus approximating the actual square symmetry by the cylindrical symmetry. With this, the solution can be written as $n(\boldsymbol{\rho})=n(\rho)e^{ij\theta}$, where j is an azimuthal index. With this form, (1) can be solved by using Bessel functions. The boundary condition can be taken as follows:

$$n(\rho)|_{\rho=\rho_0}=0 \quad (dn/d\rho|_{\rho=\rho_0}=0) \quad \text{for } j=\text{odd (even)}, \tag{2}$$

where $\rho=\rho_0$ is the boundary of the circular cell, which we take to have the same area as the actual one. The reason behind (2) is the following. Take $|j|=1$, for example. At the time $t=0$ $(\pi/2\omega)$, with the density fluctuation in each unit cell equal to $n(\rho)\cos\theta$ $[n(\rho)\sin\theta]$, the sign of charge changes as we cross the cell boundary horizontally (vertically). Hence, $n(\rho)$ at the boundary must be zero. The angular dependence of n is such that the electron gas within each unit cell forms a dipole, implying that the $|j|=1$ modes are excitable by long-wavelength electric fields. We note, for the square lattice considered here, that the symmetries of the eigenmodes are required to be those of the S, P, and D states, which form the irreducible representations of the symmetry group. These states correspond to the WS solutions with $|j|=0$, 1, and 2, respectively. Moreover, we require that $v_\rho|_{\rho=\rho_i}=0$ at the hole edge, a result of the elastic reflection of an electron from the edge. With equal angles of incidence and reflection for the edge reflection, this condition follows from taking the coarse-grain average of the electron velocity, $(1/N_e)\sum v_i$.

We solve the screened model and plot the solutions of low-lying modes in Fig. 1. They consist of three branches. Two of them, ν_+^{+1} (with $j=1$) and ν_+^{-1} (with $j=-1$), have higher frequencies than the CR; whereas the third branch, ν_- (with $j=1$), is lower in frequency than the CR. This figure contains several features observed in the experiment. Notice in particular that, near $B=0$, the ν_+^{+1} branch shows a negative B dispersion. However, there are differences between this result and the experiment. The calculated frequency of the ν_- branch saturates at high B, while the experiments observed a slightly negative dispersion in this limit, a characteristic of the edge magnetoplasmons (EMP) [5–7]. Further, besides the ν_+^{+1} branch, the theory predicts the existence of another eigenmode, ν_+^{-1}, which is degenerate with the ν_+^{+1} at $B=0$. The existence of the ν_+^{-1} mode is simply a consequence of symmetry, which can be reasoned as follows. At $B=0$, the two modes are degenerate but with opposite rotations. In the presence of B, the symmetry becomes broken, lifting the degeneracy.

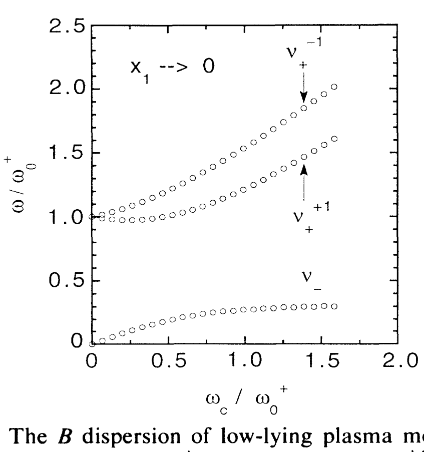

FIG. 1. The B dispersion of low-lying plasma modes in the screened approximation. ω_0^+ is the zero-field ν_+^{+1} (or ν_+^{-1}) mode frequency. The relevant parameters are $\rho_i=700$ Å and $\rho_0=1000$ Å.

Up until now, we have established a useful model that, even with several critical approximations, is able to provide a clear qualitative picture for the physics of the structures. In the actual experiments, however, the metal gates were distant from the 2DEG, and did not effectively screen the Coulomb interactions. In such and general cases, the model predicts plasma modes that are too soft. For a more quantitative understanding of the grid structures, it is essential to incorporate the effects of intracell and intercell Coulomb interactions. In view of the success of the screened model, we shall generalize it with the constraint that, in the limit $x_1 \to 0$, the generalized model reduce back to the screened one. The generalization is achieved via a variational approach.

First, we construct reasonable trial functions for $n(\boldsymbol{\rho})$ and $V_0(\boldsymbol{\rho})$. They are defined on the circular WS cell and taken to have the separable form $f(\rho)e^{ij\theta}$. By an argument parallel to the one leading to (2), we impose the conditions (we focus on the $|j|=1$ case)

$$V_0(\rho)|_{\rho=\rho_0}=0, \quad v_\rho|_{\rho=\rho_i}=0\,, \tag{3}$$

$$n(\rho)|_{\rho=\rho_0}=0\,, \tag{4}$$

which reflect the physics involved in the grid structure, i.e., the dipole formation and the edge reflection within each cell. With these functions, we can cast (1) and (3) into an integral equation. Expanding $n(\rho)=\sum c_k P_k(\rho)$, where $P_k(\rho)=(\rho-\rho_0)^k$ with $k\geq 1$, we can further write

$$V_i+(n_s e/m)(\omega^2-\omega_c^2)\sum_j G_{ij}c_j=0\,, \tag{5}$$

with $V_i=\int_{\rho_i}^{\rho_0}\rho\, d\rho\, V_0(\rho)P_i(\rho)$ and

$$G_{ij}=\int_{\rho_i}^{\rho_0}\rho_1 d\rho_1\int_{\rho_i}^{\rho_0}\rho_2 d\rho_2 P_i(\rho_1)G(\rho_1,\rho_2)P_j(\rho_2)\,,$$

where $G(\rho,\rho')$ is a Green's function. In the calculation of V_i, we incorporate e-e interactions. We create a square lattice formed with the circular WS cells, and embed the trial functions into the lattice. For $|\boldsymbol{\rho}-\boldsymbol{\zeta}_i|>\rho_0$, the functions are set to zero, where $\boldsymbol{\zeta}_i$ are the centers of the cells. We consider the e-e interactions in this artificial lattice and solve the Poisson equation in its reciprocal space, giving

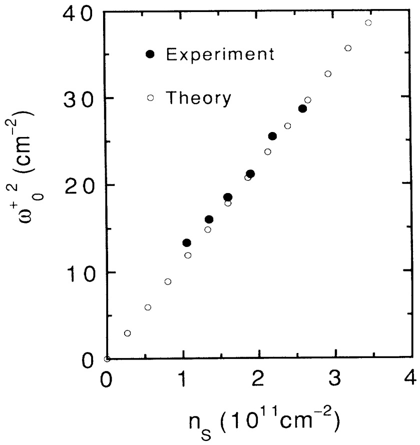

FIG. 2. The zero-field $\nu_{\mp}^{+1}$ (or $\nu_{\mp}^{-1}$) mode frequency vs the electron density for the GaAs/GaAlAs heterostructure of Zhao *et al.* [3]. The parameters used by the theory are directly taken from Ref. [3]. For the parameters not listed there, we take $\varepsilon_1 = \varepsilon_2 = 13$, and $m = 0.067 m_e$ from the CR data of the experiment.

$$V_i = -\frac{4\rho_0^2}{\pi}\sum_j \sum_{\mathbf{G}} \frac{P_j(\mathbf{G}) P_i(\mathbf{G})}{G[\varepsilon_1 \coth(G x_1) + \varepsilon_2 \coth(G x_2)]} c_j , \tag{6}$$

where $P_i(\mathbf{G})$ is the Fourier transform of $P_i(\rho) e^{ij\theta}$, and $\mathbf{G}$ is a reciprocal lattice vector. Equations (5) and (6) constitute a set of simultaneous equations for the c_j.

Numerical results have been obtained by solving (5) and (6) with eight polynomials. The zero-field $\nu_{\mp}^{+1}$ mode frequencies versus electron densities are plotted in Fig. 2. Quantitative agreement with the experiment is achieved, which supports our treatment of the Coulomb interactions.

Now, we turn to the discussion of FIR response. We shall consider only the dominant one-photon process, in which a photon is absorbed and the excited state containing a plasmon is created. In view of this, the plasma eigenmodes obtained by our model have to be quantized to properly represent the quanta of excitations (plasmons). This shall be carried out in the language of second quantization. First, we write the energy fluctuation in our model

$$H = \tfrac{1}{2} n_s m \int \mathbf{v}^2 d^2\rho + \tfrac{1}{2}\int (-e) n V_0 d^2\rho . \tag{7}$$

The eigenmodes obtained from solving (5) and (6) are inserted in (7) and quantized by requiring $H = \hbar\omega$, meaning that the energy fluctuation contained in the excited state is due to the presence of one plasmon. With the amplitudes of the fluctuations so fixed, the velocity field operator, for example, is written as

$$\hat{\mathbf{v}}(\boldsymbol{\rho}, t) = (-i/\sqrt{2}) \sum_k [\mathbf{v}_k(\boldsymbol{\rho}) \hat{b}_k(t) - \text{H.c.}] , \tag{8}$$

where $\hat{b}_k$ is the lowering operator for the kth mode, $\mathbf{v}_k(\rho)$ is the quantized velocity field, and H.c. denotes the Hermitian conjugate. The interaction Hamiltonian between a plasmon and the light can be expressed as $\hat{H}' = \int n_s(-e)\hat{\mathbf{v}} \cdot \mathbf{A}_{\text{ext}} d^2\rho$, where $\mathbf{A}_{\text{ext}}$ is the vector potential of the light. The optical matrix element $\langle 1_k | \hat{H}' | 0\rangle$ is evaluated between the ground state $|0\rangle$ and the excited state $|1_k\rangle$ containing one plasmon on the kth mode. In the FIR limit, the absorption integrated over a resonance frequency ω_k is written in terms of the matrix element as

$$\int \alpha(\omega') d\omega' \propto \frac{|\langle 1_k | \hat{\mathbf{v}} \cdot \mathbf{e} | 0\rangle|^2}{\omega_k} , \tag{9}$$

where $\mathbf{e}$ is the polarization vector of the electric field. An evaluation of $\langle 1_k | \hat{\mathbf{v}} \cdot \mathbf{e} | 0\rangle$ results in the selection rule $j = \pm 1$ for the unpolarized FIR excitation.

We compare our theory to the experiments in Figs. 3 and 4. Quantitative agreement is achieved in both cases. Notice also the appearance of slightly negative dispersion at high B in the calculation of the ν_- branch, which was

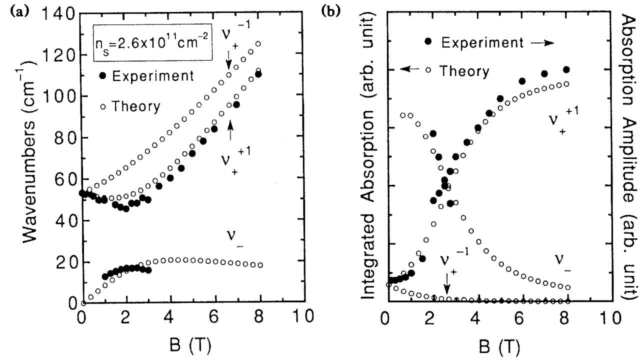

FIG. 3. (a) The left panel shows the B dispersion of low-lying modes for the GaAs/GaAlAs heterostructure of Zhao *et al.* [3]. (b) The right panel shows the absorption versus B.

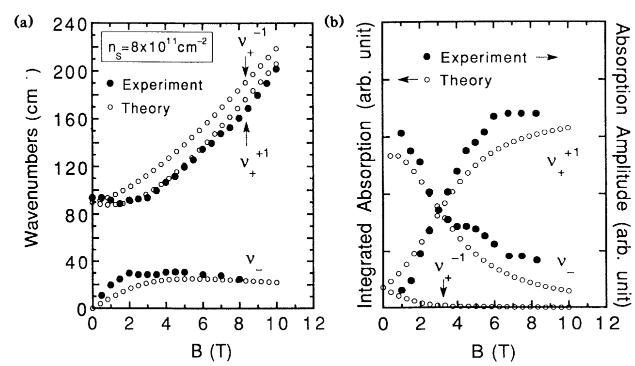

FIG. 4. (a) The left panel shows the B dispersion of low-lying modes for the InGaAs/InAlAs heterostructure of Kern *et al.* [2]. (b) The right panel shows the absorption versus B. The parameters used by the theory are directly taken from Ref. [2]. For the parameters not listed there, we take $\varepsilon_1 = \varepsilon_2 = 14$, and $m = 0.046 m_e$ from the CR data of the experiment.

absent in the screened model. As shown in Figs. 3(b) and 4(b), the absorption intensity transfers from the ν_- branch to the ν_+^{+1} branch as B increases. Notice that the ν_+^{-1} mode has a strength decreasing rapidly with B. If we assume the resonance width of the absorption is mode independent and does not change with B, the results here can be directly compared to the experimental transmission spectra, which are shown in the plots for comparison. The values of B at which the ν_- and ν_+^{+1} branches have equal strengths agree with the experiments. We have also computed for other $|j|=1$ modes with higher frequencies and found that their strengths are smaller by orders of magnitude, indicating that the oscillator strength has been exhausted by the low-lying modes [11].

In summary, we have developed a theory of the magnetoplasmons of electron grid (antidot) structures. The calculated mode frequencies and FIR absorption agree with the experiments. We interpret the interesting features of such systems as the result of an interplay of B and the unique geometry of the grid structure. It removes the existence of any $j=-1$ EMP mode, and suppresses the oscillator strength of the ν_+^{-1} mode, as it has the opposite sense of rotation to the cyclotron motion. On the other hand, the ν_+^{+1} mode and the ν_- mode, having the same sense, can share the oscillator strength.

After completing the calculation, we heard of the work by Lorke, Jejina, and Kotthaus [12] on numerical simulations of LSLs, within a classical, single-particle model of ballistically moving electrons, which is entirely different from our collective approach. They claim that the single-particle model contains qualitative features of the long-wavelength dynamic response, and suggest a generalized Kohn theorem for the LSLs.

We are grateful to Professor D. C. Tsui for many valuable discussions and for his constant support during this work. We also acknowledge discussions with Professor L. J. Sham. One of us (G.Y.W.) thanks Princeton University for the hospitality received during his visit, and the NSC of ROC for sponsoring the visit. This work is supported by the AFOSR under Grant No. AFOSR-91-0353.

*On leave from Department of Electrical Engineering, Tsing-Hua University, Hsin Chu, Taiwan 300, Republic of China.

[1] W. Kohn, Phys. Rev. **123**, 1242 (1961); L. Brey, N. F. Johnson, and B. I. Halperin, Phys. Rev. B **40**, 10647 (1989).

[2] K. Kern, D. Heitmann, P. Grambow, Y. H. Zhang, and K. Ploog, Phys. Rev. Lett. **66**, 1618 (1991).

[3] Y. Zhao, D. C. Tsui, M. Santos, M. Shayegan, R. A. Ghanbari, D. A. Antoniadis, and H. I. Smith, Appl. Phys. Lett. **60**, 1510 (1992).

[4] R. Fleischmann, T. Giesel, and R. Ketzmerick, Phys. Rev. Lett. **68**, 1367 (1992), and references therein.

[5] D. B. Mast, A. J. Dahm, and A. L. Fetter, Phys. Rev. Lett. **54**, 1706 (1985); A. L. Fetter, Phys. Rev. B **33**, 5221 (1986).

[6] D. C. Glattli, E. Y. Andrei, G. Deville, J. Poitrenaud, and F. I. B. Williams, Phys. Rev. Lett. **54**, 1710 (1985).

[7] J.-W. Wu, P. Hawrylak, and J. J. Quinn, Phys. Rev. Lett. **55**, 879 (1985).

[8] C. C. Grimes and G. Adams, Phys. Rev. Lett. **36**, 145 (1976); S. J. Allen, D. C. Tsui, and R. A. Logan, Phys. Rev. Lett. **38**, 980 (1977); A. Lorke, J. P. Kotthaus, and K. Ploog, Phys. Rev. Lett. **64**, 2559 (1990); T. Demel, D. Heitmann, P. Grambow, and K. Ploog, Phys. Rev. Lett. **66**, 2657 (1991), and references therein.

[9] An estimate by using the experimental parameters obtains $\lambda \gg a^*$, where a^* is the effective Bohr radius, justifying the neglect of compressibility effects.

[10] The original WS method was developed to study the S states of metal band structures. See E. Wigner and F. Seitz, Phys. Rev. **43**, 804 (1933).

[11] The optical absorptions in the screened model display the same patterns of variations with B as discussed in this paragraph.

[12] A. Lorke, I. Jejina, and J. P. Kotthaus, Phys. Rev. B **46**, 12845 (1992).